Transactions of the Materials Research Society of Japan 26 [3] 985-988 (2001)

Physical properties of the SrO- and TiO_2- terminated $SrTiO_3$(100) surface

T. Kubo and H. Nozoye*
National Institute of Materials and Chemical Research, 1-1 Higashi, Tsukuba, Ibaraki 305-8565, Japan
Phone: +81-298-61-4527, Fax: +81-298-61-4504, e-mail: nozoye@nimc.go.jp

Local physical properties of a $SrTiO_3$(100) surface were studied by using scanning tunneling microscopy (STM) and non-contact atomic force microscopy (NC-AFM). Comparing with the results of *ab initio* calculations, SrO- and TiO_2- terminated domains were identified. The electronic band gaps for the SrO- and the TiO_2- domains were observed to be about 1.4 (1.75) and 0.6 (1.31) eV, respectively (calculated values). The work function for the SrO domain was observed to be lower by 0.2 eV than that of the TiO_2 domain, which was also relatively consistent with the calculations. The sample bias voltage dependent changes in the AFM images, which were related to the differences in the local work function, were observed.
Key words: STM, NC-AFM, Metal Oxides, Surface Morphology

1. INTRODUCTION

Strontium Titanate ($SrTiO_3$) has been of interest because of its catalytic activities, dielectric properties and a lattice-matched substrate for high-*Tc* oxide superconductors. It has been studied intensively by use of many experimental techniques and theoretical methods [1-10]. As perovskite $SrTiO_3$ with a cubic structure is composed of SrO- and TiO_2- alternative layers in the <100> direction, the (100) surface can be terminated by either SrO- or TiO_2- domain. The surface physical and chemical properties must be greatly influenced by the ratio of these two kinds of terminated domains. Fompeyrine et al. reported the morphology of two terminated domains on a $SrTiO_3$(100) surface by use of scanning friction microscopy (SFM) [4]. The friction constant on a SrO- domain was observed to be about 3/2 times larger than that on a TiO_2- domain, however, local physical properties of these domains have not been well understood. Scanning Kelvin probe microscopy (SKPM) using non-contact atomic force microscopy (NC-AFM) has an advantage to observe atomic level images and the tip-sample interaction simultaneously. Analysis of the tip-sample interaction, such as electrostatic, magnetic and chemical forces etc., allows us to obtain information about local properties of the surface. Further, by simultaneous use of scanning tunneling microscopy (STM), we can get information about a local electronic property.

In this study, the surface morphology and the local physical properties of the SrO- and the TiO_2- domains on a $SrTiO_3$(100) surface were studied by use of SKPM and STM. Comparing with the results of *ab initio* calculations, the terminated domains were identified. The sample bias voltage dependent changes in the topography of AFM images, which were related to the differences in the local electrostatic property between SrO- and TiO_2- terminated domains, were observed.

2. EXPERIMENTAL

Experiments were carried out in an ultra high vacuum non-contact AFM (UHV non-contact AFM; JEOL model JAFM-4400) with a base pressure of $\leq 1.4 \times 10^{-8}$ Pa. Cone-shaped silicon cantilevers with f_0=140-290 kHz and k=4-14 N/m (Silicon-MDT Ltd.) were used for AFM measurement. The cantilever was highly doped with B (0.002 Ωcm) and coated with W_2C (25 nm thick, 30 μΩcm). AFM measurements were performed either in the constant force condition or the spectroscopic sequence. Tips used for STM measurements were the same cantilevers or 0.3 mm diameter tungsten tips, which were made by electrochemical etching in 2N KOH solution. STM measurements were performed either in the constant current condition or the spectroscopic sequence.

In order to obtain a smooth surface, a $SrTiO_3$(100) substrate of $7 \times 1 \times 0.5$ mm^3 (Nakazumi crystal Co. Japan) was first treated with a buffered NH_4F-HF (BHF) solution (pH=4.5 and NH_4F concentration of 10M) for 10 min [2], then polished by using colloidal diamond paste (<0.1 mm). The sample was directly mounted on a silicon heater. Vacuum pressure during annealing did not exceed 5×10^{-7} Pa. Temperature was measured with an optical pyrometer. After heating at 1000 °C, color of the sample became slightly dark, and the sample had some conductivity for STM measurements.

3. CALCULATION METHOD

The calculations based on density function theory (DFT) were performed using an *ab initio* ultrasoft pseudopotential with a plane-wave basis. In this method, valence electron wave functions were obtained by minimizing the Kohn-Sham total-energy function [11]. The exchange correlation potential was treated with the generalized gradient approximation (GGA) [12]. The self-consistent ultrasoft pseudopotential proposed by Vanderbilt [13] was used for electron-ion interaction. A plane wave cut off of 260 eV and Monkhorst-Pack [14] of (5,5,1) were used.

SrO- and TiO_2- terminated surfaces of $SrTiO_3$(100) were modeled by periodic slabs. Each slab consisted of seven alternatively stacked atomic layers of SrO and TiO_2 and was isolated by $2 \times a_{STO}$ width of vacuum regions. Atoms at central three layers were fixed at the bulk position, on the other hand, all other atoms were geometry optimized. The criterions of energy change per atom, RMS displacement of atoms and RMS force on

each atom were 5×10^{-6} eV, 5×10^{-4} A and 0.05 eV/A, respectively. Gaussian smearing of 0.2 eV was used.

4. RESULTS AND DISCUSSION

Figure 1a shows an STM image of a 500×500 nm^2 region of $SrTiO_3$(100) after heating at 1080 °C for 5 min. The image shows that the surface is composed of large terraces, steps and rectangular domains. Most of the steps were observed along [010] or [001] directions. Fompeyrine et al. reported that TiO_2- terminated terrace edges meander along [010] and [001], whereas SrO-terminated terrace edges are curved with a radius of 70-300 nm [4]. These two kinds of step morphologies were not clearly observed in our study. The morphology of the step direction is strongly influenced by annealing conditions and initial sample preparations [2-4,7-10], perhaps, our experimental conditions were different from theirs. The step heights along a line a-b are about 0.4 nm, which corresponds to a unit cell length (a_{STO}=0.3905nm) of bulk $SrTiO_3$, as shown in Fig. 1b. As the $SrTiO_3$(100) surface is composed of SrO- and TiO_2- alternative layers with the distance of $a_{STO}/2$, the lower region and the higher large terraces along the line a-b are terminated by the same layer. These are tentatively denoted by domain A. On the other hand, the step heights along a line c-d are about 0.2 nm, which corresponds to a half unit cell length, suggesting that the lower region (denoted by B) along the line c-d is terminated by another layer. Each step height was multiples of the half unit cell length ($a_{STO}/2$), respectively. Each domain can be labeled by either A or B. It is noted that all of the large terraces are terminated by domain A, and the rectangular domains are terminated by domains A or B.

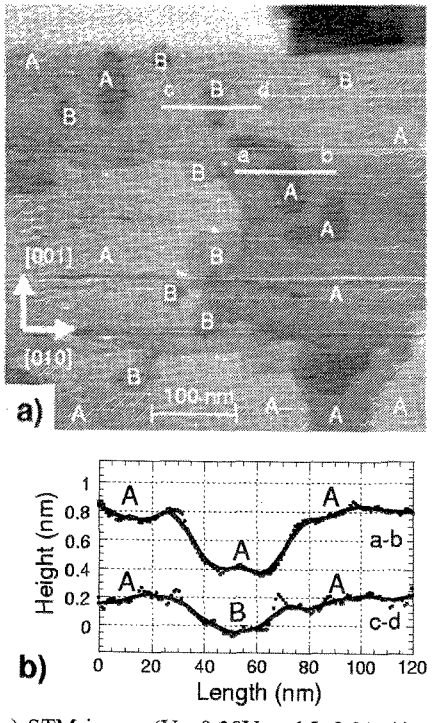

Fig. 1 (a) STM image (V=-0.38V and I=0.01nA), using a W-tip, of $SrTiO_3$(100) of 500×500 nm^2 region after heating to 1080 °C for 5 min. (b) The vertical profiles along lines a-b and c-d.

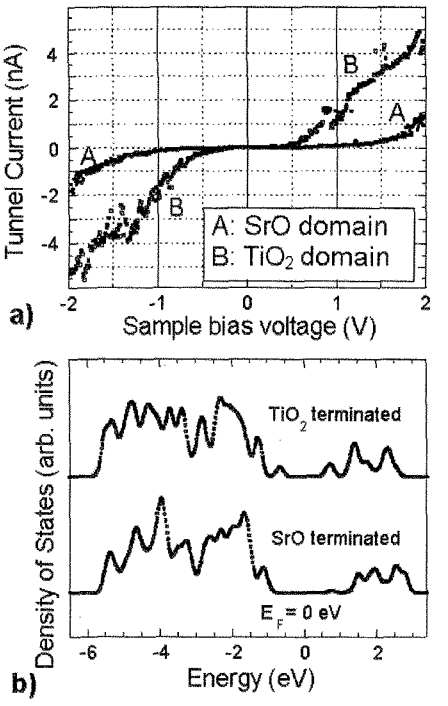

Fig. 2 (a) *I-V* characteristics for domains A and B of $SrTiO_3$(100). (b) Calculated density of states for the SrO- and the TiO_2- terminated slabs.

In order to identify surface terminations (SrO or TiO_2), *I-V* properties were measured for each domain, as shown in Fig. 2a. Although the *I-V* properties had some inhomogeneous behavior, the electronic energy band gap for the domain A (~1.4 eV) is relatively larger than that of domain B (~0.6 eV). As the sample was heated at high temperature, the concentration of oxygen vacancy increased. The inhomogeneous behavior of *I-V* properties may be influenced by the inhomogeneous distribution of oxygen vacancy.

Calculated density of states for relaxed SrO- and TiO_2- terminated $SrTiO_3$(100) slabs, by first-principles total-energy calculations, are shown in Fig. 2b. The electronic energy band gaps for the SrO- and the TiO_2-terminated slabs were estimated to be 1.75 and 1.31 eV, respectively. These values are seemed to be consistent with published results of 2.11 and 1.83 eV reported by Li et al. [5], and 1.86 and 1.13 eV reported by Padilla and Vanderbilt [6]. Comparing with the experimental values, it is concluded that the domains A and B are terminated by the SrO- and the TiO_2- layers, respectively.

Figure 3 shows calculated optimized structures for a) SrO- and b) TiO_2- terminated $SrTiO_3$(100). At the surface layer, all atoms are pushed into the substrate compared with the ideal surface, and the Sr and Ti atoms move deeper than oxygen atoms, Δ(Sr-O)=0.19 Å and Δ(Ti-O)=0.11 Å, leading to the surface rumpling. The changes of the interlayer spacing between the first and the second layers, and the second and third layers are -5.9 % (SrO) and -5.5 % (TiO_2), and +3.1 % (SrO) and +7.4 % (TiO_2), respectively.

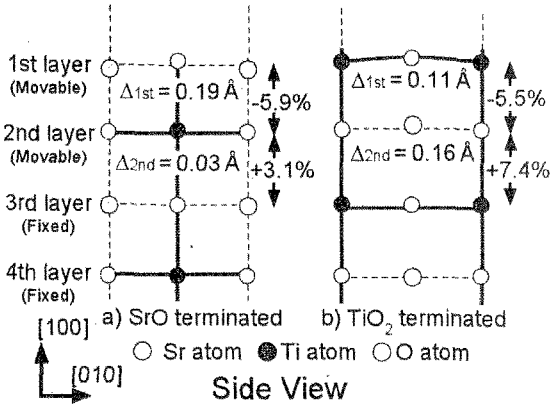

Fig. 3 The optimized structures for a) SrO- and b) TiO_2-terminated $SrTiO_3$(100).

Figure 4a shows an AFM image (740×740 nm^2) of the same sample as shown in Fig. 1a. Schematic of the image is shown in Fig. 4d. Two types of rectangular domains (bright and dark domains) were observed. The depth of the dark contrast was several Å. On the other hand, the height of the bright domain was several tens of Å, suggesting that additional force such as electrostatic force acted on the cantilever. When there is a potential difference U between the cantilever and the sample, the electrostatic force between them is expressed as:

$$F = -1/2U^2 \partial C/\partial Z$$

Where C and Z are effective capacitance and distance between the cantilever and the sample, respectively [15]. In the present study, all AFM measurements were performed in constant force condition. When electrostatic force is additionally applied, the cantilever will be retracted by the distance of S in order to avoid the additional force. If the local work function of the bright domain is different from that of the dark domain, the force induced by electrostatic field is also different. Figure 4d shows the *S-V* property of each domain. The sample bias of the minimum point indicates the contacts potential difference between the cantilever and the surface domain. The contact potential difference of the terrace and the dark domain was the same (curve A), which was lower by 0.2 V than that of the bright domain (curve B). Because the large terraces are terminated by the SrO layer, the bright domain (B) and the dark domain (A') must be terminated by the TiO_2- and the SrO- layer, respectively. As the same cantilever was used during the measurements, the work function for the SrO domain (Φ_{SrO}) is lower by 0.2 eV than that of the TiO_2 domain (Φ_{TiO2}). The calculated work functions (Φ) for SrO- and TiO_2- terminated slabs were 4.9 and 7.1 eV, respectively. The values were overestimated comparing with the expected value of 4.2 eV (experimental) [1], however, the calculated results ($\Phi_{SrO} < \Phi_{TiO2}$) are relatively consistent with our *S-V* results. It is noted that the *S-V* property of the region A (A') was always the same, on the other hand, that of the region B slightly depended on its domain size. Because the size of the region B (below several tens of nm) and the radius of the tip of cantilever (~10 nm) are nearly the same and Coulomb force is long-range force, the *S-V* property of the region B may be somewhat influenced by the surrounding region A. These suggest that actual contact potential difference between the TiO_2- and the SrO-terminated regions may be a little bit larger than 0.2 eV.

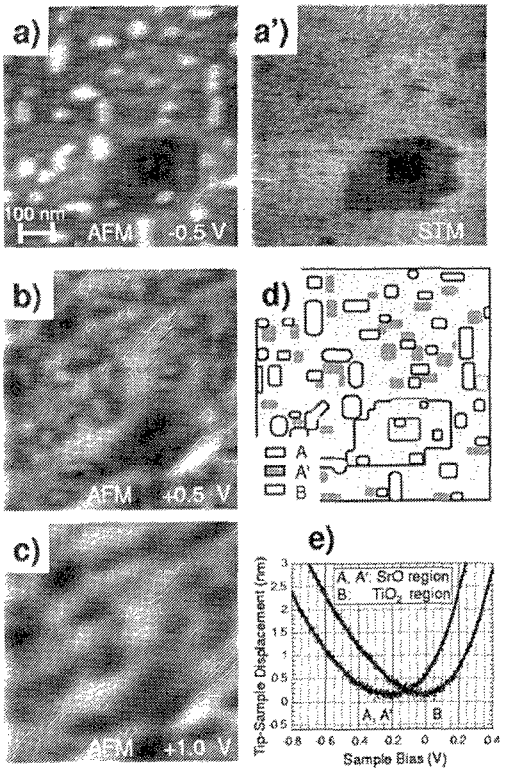

Fig. 4 (a-c) Sample bias voltage dependent AFM images of $SrTiO_3$(100) of 720×720 nm^2 region after heating to 1080 °C for 5 min. (a') STM (V=-0.46V and I=0.12A) images, using the same cantilever, of $SrTiO_3$(100) of 720×720 nm^2 region after heating to 1080 °C for 5 min. (d) Schematic of the surface morphology. (e) *S-V* characteristics for domains A and B (frequency shift of ~50Hz).

Figure 4a' shows an STM image of the same surface area using the same cantilever. The dark rectangular domains, which were observed in AFM measurements, were clearly observed, on the other hand, the bright rectangular domains were poorly observed. These indicate that the step height between the dark domain and the terrace is higher than that between the bright domain and the terrace. This suggests that the dark domains are the same termination with the terrace (step height of $2\times a_{STO}/2$), on the other hand, the termination of the bright domains is different from that of the terrace (step height of $1\times a_{STO}/2$). It is also consistent with our AFM and *S-V* results.

The sample bias voltage dependent AFM images of the $SrTiO_3$(100) surface were shown in Fig 4a-c. The TiO_2 terminated domains were observed as bright contrast at the sample bias voltage of -0.5 V (Fig. 4a). However, at V=+0.5 V (Fig. 4b), the bright domains were surrounded by dark peripherals. Further, at V=+1.0 V (Fig. 4c), the TiO_2 terminated domains were observed as dark contrast. Similar bias voltage dependent AFM results of surface charge on GaAs(110) have been reported by Sugawara et al. [16]. In this case, the work

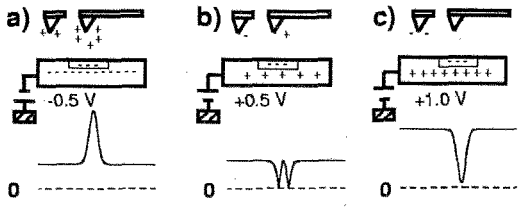

Fig. 5 Models and electrostatic force profiles to explain the sample bias voltage dependence [16].

function of the TiO_2 domain is slightly higher than that of the SrO domain, the TiO_2 domain induces relatively positive charge on the cantilever. It is equivalent that relatively negative charge is located on the TiO_2 domain, comparing with the SrO domain. Models and electrostatic force profiles to explain the sample bias voltage dependence [16] are shown in Fig. 5. As for the negative voltage image, the negative charge, located in the substrate, induces the positive charge on the cantilever. Electrostatic force depends on the amounts of the charge induced on the cantilever. As for the positive voltage image, the positive charge, located in the substrate, induces the negative charge on the cantilever. However, at the negatively charged TiO_2 domain, the positive charge will be induced on the cantilever. At the near edge of the TiO_2 domain, no charge is induced on the cantilever, suggesting that no electrostatic force exists applied. Then, the TiO_2 domain seem to be surrounded by the dark peripherals. Domain contrast between two kinds of terminations has been clearly observed in AFM images. SKPM using NC-AFM is capable of distinguishing differently terminated domains on the $SrTiO_3$(100) surface.

5. CONCLUSION

Local physical properties for the SrO- and TiO_2-terminated domains on the $SrTiO_3$(100) surface were studied by use of STM and NC-AFM. Comparing with the results of *ab initio* calculations, the terminated domains were identified. The electronic band gaps for the SrO- and TiO_2- domains were observed to be about 1.4 and 0.6 eV, respectively. The work function of the SrO terminated domain was lower by 0.2 eV than that of the TiO_2 terminated domain. KSPM is capable of resolving charges in electric-field distribution between the SrO- and TiO_2- terminated domains on the $SrTiO_3$(100) surface.

Acknowledgements: This work was supported in part by Grants-in-Aid from the Science and Technology Agency.

References

[1] Y.-W. Chung, W.B. Weissbard, Phys. Rev. B20, 3456 (1979).
[2] M. Kawasaki, K. Takahashi, T. Maeda, R. Tsuchiya, M. Shinohara, O. Ishiyama, T. Yonezawa, M. Yoshimoto, H. Koinuma, Science 266, 1540 (1994).
[3] B. Stauble-Pumpin, B. Ilge, V.C. Matijasevic, P.M.L.O Scholte, A.J. Steinfort, F. Tuinstra, Surf. Sci. 369, 313 (1996).
[4] J. Fompeyrine, R. Berger, H.P. Lang, J. Perret, E. Machler, Ch. Gerber, J.-P. Locquet, Appl. Phys. Lett., 72, 1697 (1998).
[5] Z.-Q. Li, J.-L. Zhu C.Q. Wu, Z. Tang, Y. Kawazoe, Phys. Rev. B58, 8075 (1998).
[6] J. Padilla, D. Vanderbilt, Surf. Sci. 418, 64 (1998).
[7] M. Lippmaa, K. Takahashi, T. Ohnishi, S. Ohashi, N. Nakagawa, A. Ohtomo, T. Sato, M. Iwatsuki, H. Koinuma, M. Kawasaki, Proceedings of the Second Symposium on Atomic-scale Surface and Interface Dynamics 205 (1998).
[8] J. Nie, A. Shoji, M. Koyanagi, H. Takashima, N. Terada, K. Endo, Jpn. J. Appl. Phys. 37, L1014 (1998).
[9] H. Tanaka, H. Tabata, T. Kawai, Thin Solid Films 342, 4 (1999).
[10] K. Szot, W. Speier, Phys. Rev. B60, 5909 (1999) .
[11] W. Kohn, L.J. Sham, Phys. Rev. 140, A1133 (1965).
[12] J.P. Perdew, Physica B172, 1 (1991).
[13] D. Vanderbilt, Phys. Rev. B41, 7892 (1990).
[14] H.J. Monkhorst, J.D. Pack, Phys. Rev. B13, 5188 (1976).
[15] S. Kitamura and M. Iwatsuki, Appl. Phys. Lett. 72, 3154 (1998).
[16] Y. Sugawara, T. Uchihashi, M. Abe, S. Morita, Appl. Surf. Sci. 140, 371 (1999).

(Received November 22, 2000; Accepted December 25, 2000)